
From AGB Stars to Planetary Nebulae – How the Journey Begins

Raghvendra Sahai

Jet Propulsion Laboratory, California Institute of Technology, MS 183-900, 4800
Oak Grove Drive, Pasadena, CA-91109 sahai@jpl.nasa.gov

Summary. Pre-Planetary Nebulae (PPNe) have traditionally been understood as rare objects that represent a transitory phase in the evolution of AGB stars to planetary nebulae (PNe). Recently, mainly due to high-resolution imaging surveys with HST, it has become possible to start studying the detailed physical properties for a sufficient number of these objects. The results from several surveys with HST (and supporting ground-based observations) conducted using candidate lists of PPNe based on a very simple IRAS 25-to-12 μ m color criterion, show objects with a wide range of morphologies, similar to those seen in young PNe. A modified version of this color criterion has been used to select nascent PPNe (nPPNe), i.e. objects just beginning their transition from the AGB to the PPN phase. Imaging results from an HST survey of nPPNe support the idea that the journey of an AGB star towards an aspherical PPN is initiated by the launching of fast collimated outflows.

Key words: pre-planetary nebulae, planetary nebulae, stars: AGB and post-AGB, mass-loss, circumstellar matter

1 Introduction

The fundamental question which has motivated this series of conferences on Asymmetrical Planetary Nebulae, may be stated as follows – how do the slowly expanding (5-15 km s⁻¹), largely spherical, circumstellar envelopes (CSEs) of AGB stars transform themselves into highly aspherical Planetary Nebulae (PNe), which show collimated lobes and fast outflows (\gtrsim few \times 100 km s⁻¹) along one or more axes.

Until at least the late 1990's, a widely accepted answer to this question was provided by the Generalized Interacting Stellar Wind model (GISW) [1], in which a very fast (\gtrsim 1000 km s⁻¹) spherical, radiatively-driven wind from central star of the PN interacts with an equatorially dense AGB wind, producing a wide variety of axisymmetric shapes [2, 19, 9, 7]. However, based on the wide variety of multipolar and point-symmetric morphologies seen in unbiased surveys of young PNe with HST, Sahai & Trauger proposed in 1998 that collimated fast winds or jets (hereafter CFWs), operating during the PPNe or very late-AGB phase, are the primary agent for producing asymmetric shapes in PNe[22]. The CFWs are likely to

be episodic, and either change their directionality (i.e., axis wobbles or precesses) or have multiple components operating in different directions (quasi)simultaneously. These CFWs sculpt the AGB CSE from the inside-out, producing elongated bubbles or lobes within the CSEs. Later, additional action of the fast radiative wind from the central star may further modify these lobes, and ionization may lead to loss of some structure. If a dense equatorial torus is present, it may add additional confinement for the CFWs, as well as for the spherical radiative wind from the hot central star at a later stage of evolution. Theoretical models have been presented for producing disks/tori and jet-like outflows in a binary system either via (i) common-envelope evolution [29] or (ii) formation of an accretion disk due to Bondi-Hoyle accretion of the AGB wind [16].

Thus although the basic idea that the shaping of PNe involves interacting winds [12] is correct, the idea that hydrodynamical collimation of the fast wind by an aspherical slow one, is the primary shaping mechanism, is probably not. And primary shaping begins *prior* to the PN phase, as surveys of PPNe so vividly demonstrate [25]. The morphological data suggests that the fast outflows are probably born collimated (i.e. collimated at or very near the launch site). Fast ($\text{few} \times 100 \text{ km s}^{-1}$) molecular bipolar outflows in PPNe and a few late AGB stars with large momentum-excesses indicate that these winds are not radiatively driven [3]. This review focuses on observations which probe the innermost regions of the CSEs in order to trace the very beginnings of the journey of an AGB CSE towards an aspherical PPNe/PN.

2 Ground-Based Techniques: A Brief History

I first briefly review the high-resolution ground-based techniques (all at near-infrared wavelengths) which have been used to study AGB stars and related objects since the 1980's. E.g., with a 4m aperture, at $2.2 \mu\text{m}$, one can hope to resolve structures on the 100 mas scale with diffraction-limited imaging. However, special techniques are needed to achieve the latter due to the presence of atmospheric seeing which normally limits our angular resolution to about $1''$. These techniques include:

(1) *Speckle Interferometry* (in which seeing-induced fluctuations are "frozen" by recording images quickly, but variable seeing is a major limitation) – e.g., 1.6-4.8 μm spatial visibility data for 16 objects revealed deviations from spherical symmetry for the "most resolved" objects [6].

(2) *Single-Baseline Interferometry* (e.g. with the Infrared Spatial Interferometer ISI at Mt. Wilson by the Townes group, e.g. [5]) – the major limitations of this technique have been (a) insufficient u-v coverage for measuring the complex visibility function (whose Fourier-transform yields the source brightness distribution), thus limiting one to simple model-fitting in terms of core/halo structures and (b) insufficient dynamic range.

More recently, *Sparse-Pupil* (also known as *Aperture-Masking Interferometry*) (with much improved u-v coverage, and closure phase information) has enabled higher fidelity maps of the brightness distribution in the near-infrared (e.g., [30, 15]). In addition, NIR Adaptive Optics (AO) observations (e.g. with NACO/VLT [14] or Keck [17]) and mid-IR imaging with large apertures (e.g. with TIMMI/ESO3.6m [13]) have also begun to provide diffraction-limited images. 3-element interferometers are now operating (IOTA in the NIR: [18]; ISI in the mid-IR: [31]) which provide closure phase data and thus more reliable detection of asymmetries in the dust shells

and/or the extended stellar atmosphere, but still lack the capability to provide real images.

3 Detailed Studies of nPPNe with HST

The high spatial resolution ($0''.1$ at R-band), stable PSF, and very high dynamic range afforded by HST's ACS (and WFPC2 and STIS in the past) instruments makes it the facility of choice for studying nPPNe. We first summarize results from such studies of 4 key nPPNe. We do not include the well-known object OH231.8+4.2 (with an M9III central star) in this list because it is already a well-developed PPN, the expansion age of the nebular lobes being ~ 500 – 800 yr.

1. *V Hydrae*, a cool carbon star with fast molecular outflows [21, 11] and optical emission lines, was observed with HST's long-slit spectrograph STIS, in order to probe the spatio-kinematic structure of its high-velocity outflow very close to the central star [24]. The multi-epoch imaging (over a 1-year period) showed a very fast (projected radial velocity 240 km s^{-1}) blobby outflow, which is evolving very quickly, as well as a central, expanding (at 10 km s^{-1}) disk (diameter $0''.5$) in $\text{H}\alpha$ emission. An extended, slowly expanding torus was found from CO J=1-0 interferometric data (OVRO). The torus and high-velocity outflows have also been mapped with the SMA [8].

2. *IRC+10216* is the most well-studied carbon star, with a massive, slowly expanding CSE. Archival HST images taken with WFPC2 and NICMOS show three main features (a) a Southern cone, (b) a North double-fan, and (c) a dark waist separating features *a* and *b* (Fig. 1). A simple model of the source comprising of an equatorially-dense inner region and a spherical outer region is clearly inadequate at reproducing the observed images [28]. Sparse Pupil interferometry on Keck I has been used to reconstruct K-band images (but without astrometric information) of the central $0''.5$ with diffraction-limited resolution (~ 50 mas) showing complex, blobby structure [30]. Unfortunately it is difficult to find a one-to-one correspondence between the HST and K-band images, except for the bright Southern cone.

3. *CIT 6* is another very well-studied carbon star with a massive, slowly expanding CSE. WFPC2/HST imaging in the *b*, *v*, and *r* filters shows 2 compact cores separated by $0''.15$ (60 AU) along $\text{PA} \sim 15^\circ$ with a dark E-W waist separating them [27]. The N-core is very red. A broad fan-structure opens to the north, stretching to $2''.5$, and a narrow blue fan is directed eastwards. At $1.1 \mu\text{m}$, nebulosity extends out to about $25''$ at a $\text{PA} \sim 30^\circ$. 2.2 and $3.1 \mu\text{m}$ sparse-pupil interferometric imaging of the central 200 mas shows a central bright core which is extended along $\text{PA} \sim 107^\circ$, and a fainter, extended nebula roughly orthogonal to the core [15]. A $9.7 \mu\text{m}$ image with the ESO 3.6m/TIMMI camera shows a teardrop shape of size about $8''$, elongated along the same PA as the faint nebulosity seen most clearly in the $3.1 \mu\text{m}$ image [13].

4. *IRC+10011* is a very red oxygen-rich star with a massive, slowly expanding CSE, and was imaged in our PPN survey [25]. The $0.8 \mu\text{m}$ image shows a central, asymmetrical, elongated (oval-shaped) nebulosity; the peak brightness region is also elongated and non-stellar and the position angles of the elongations seen on small and large scales are different.

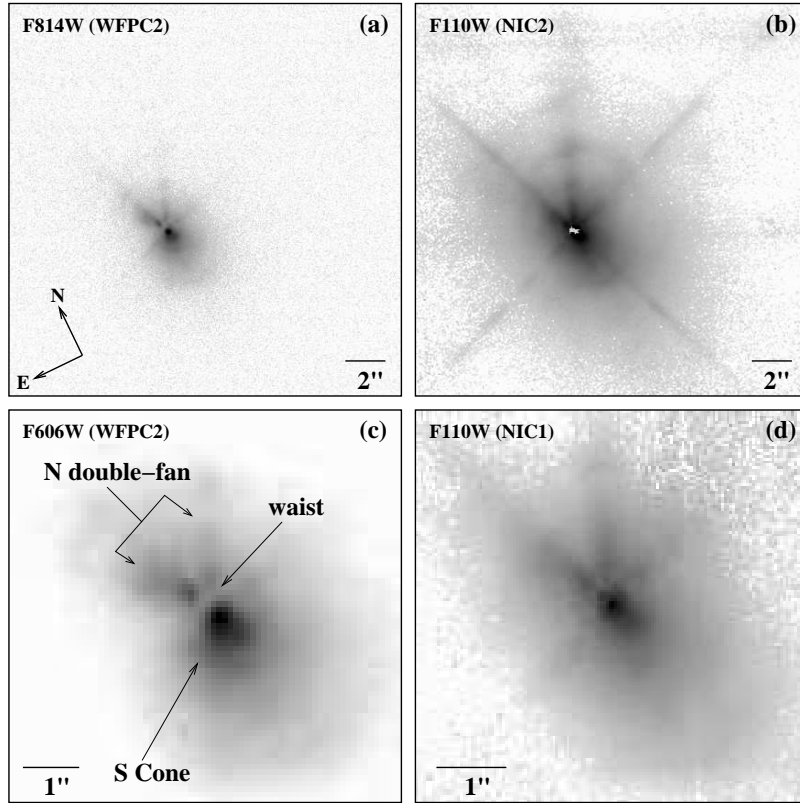


Fig. 1. HST images of the nPPN, IRC+10216. The bottom panels show magnified views of the central region

3.1 New HST Survey for nPPNe

A star begins its post-AGB journey when heavy AGB mass-loss process ceases. At roughly the same evolutionary phase, observational evidence shows that a fast outflow starts excavating a cavity from the inside out. In either case, due to the resulting lack of hot dust (compared to a star with ongoing heavy mass-losing) thermal emission at short ($\lesssim 10 \mu\text{m}$) wavelengths, relative to that at longer wavelengths ($\gtrsim 25 \mu\text{m}$), will decrease. Thus the IRAS 25 to $12 \mu\text{m}$ flux ratio, F_{25}/F_{12} , provides a simple method to pre-select candidate nPPN objects from, e.g., CO catalogs of AGB stars. Since we had already very successfully utilized this color criterion to select PPNe from catalogs of OH/IR stars ($F_{25}/F_{12} > 1.4$), we simply modified it to select nPPNe: we chose objects with $F_{25}/F_{12} > 0.33$ and < 0.67 . Figure 2 shows F_{25}/F_{12} computed for a spherical AGB mass-loss envelope with a central cavity using dust radiative-transfer models – it increases monotonically from a value of 0.3 for a filled envelope to larger values as the size of the cavity increases. Note that a 100 km s^{-1} outflow will excavate a lobe of radius $\lesssim 1500 \text{ AU}$ (i.e. $0.75''$ - $0.5''$ for an object at a typical distance of 2–3 kpc) in 75 yr. The “water-fountain” nebulae

such as IRAS 16342-3814, IRAS19134+2131 and W43A PPNe are examples of such young PPNe[4]. Our survey [26] was directed towards finding objects which are in transition to the PPN phase, but even younger than these PPNe.

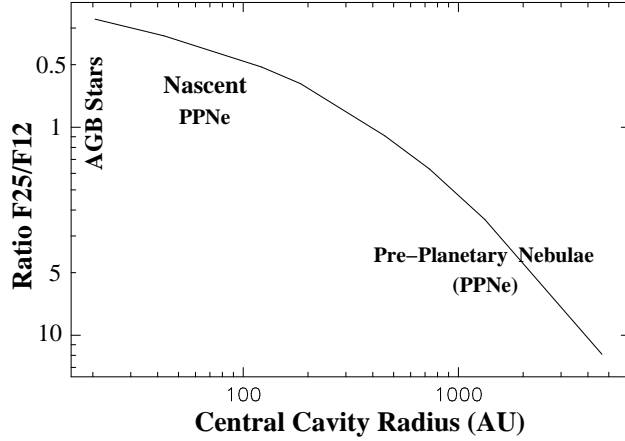


Fig. 2. The 25 to 12 μ m flux ratio, as a function of the radius of a central cavity in a spherical AGB mass-loss envelope, computed using DUSTY [10] radiative-transfer models. (Note reversed scale for y-axis.)

4 Results

Out of a total of 48 objects imaged, compact, but non-stellar, morphologies are seen in at least 25% (compared to 50% in PPN survey)(e.g., Figs. 3, 4). The remaining objects are either unresolved, or only marginally resolved. Detailed PSF subtraction/removal has not been completed for these objects – thus some of the marginally resolved objects may be found to possess extended structure. Aspherical structure is seen in the resolved objects. In some objects, a diffuse, round, halo is also seen, representing the undisturbed AGB mass-loss envelope. A few sources show discrete circular (partial) arc-like features.

The aspherical structure in nPPNe is different from that observed in PPNe, which generally show limb-brightened, roughly equal-sized lobes on both sides of the center. In contrast, only one-sided structures are seen in our survey nPPNe. This could be due to either the structures being intrinsically (i) one-sided, or (ii) bipolar, but with only near-side being visible due to the much higher circumstellar obscuration in these objects (compared to normal PPNe) hiding the far-side component from view.

The observed structures in nPPNe could result from either (a) an aspherical density distribution in the imaged region, and/or (b) aspherical illumination. Case (b) requires the presence of relatively low-density channels close to the central star,

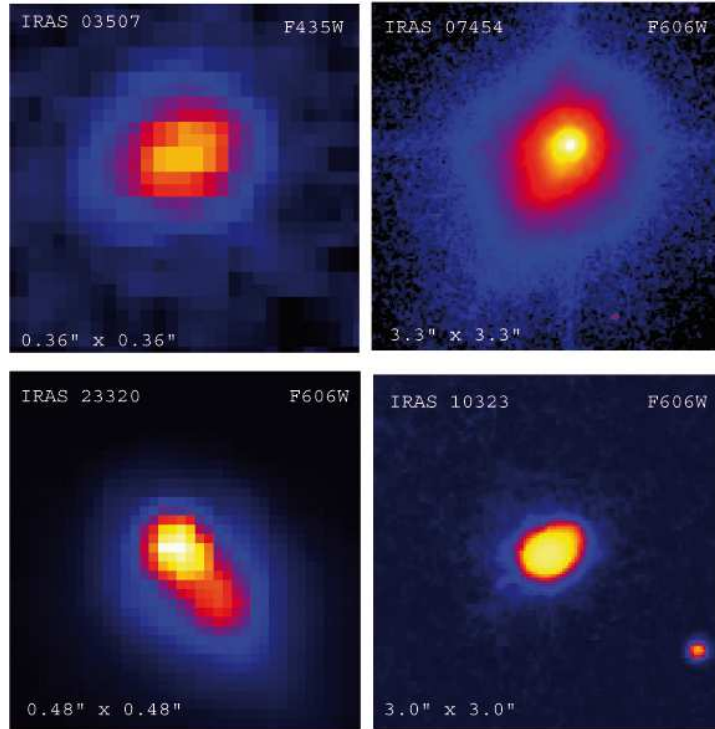


Fig. 3. HST images of nPPNe (*adapted from [26]*)

which allow the starlight to escape preferentially along specific directions, and illuminate more distant regions of the circumstellar medium in an aspherical manner. The searchlight beams and polar lobes of the Egg Nebula[23] provide an example where both case (a) and (b) apply.

5 Conclusions

Although our current sample of nPPNe is too small for general conclusions, our survey results, together with detailed studies of 4 nPPNe, support the hypothesis that the mechanism for creating the large-scale density inhomogeneities are high velocity outflows carving the AGB mass-loss envelope from the inside out. In order to test this hypothesis, we need kinematic data on small scales, e.g., using mm-wave interferometry of high-excitation molecular lines, such as SiO, CS, high-J CO lines with ALMA; or the $4.6\mu\text{m}$ CO lines with a coronagraph to mask the very bright continuum from the central source [20]. The change in PA from small to larger scales (as e.g., in IRC+10011, CIT6 and IRAS 15082) or multi-axial elongations as in IRAS 18560 suggests that the outflows change direction (or multiple outflows are present simultaneously). The outflows are probably not single-velocity, smooth and continuous (note, e.g., the blobby structure and multiple kinematic components in

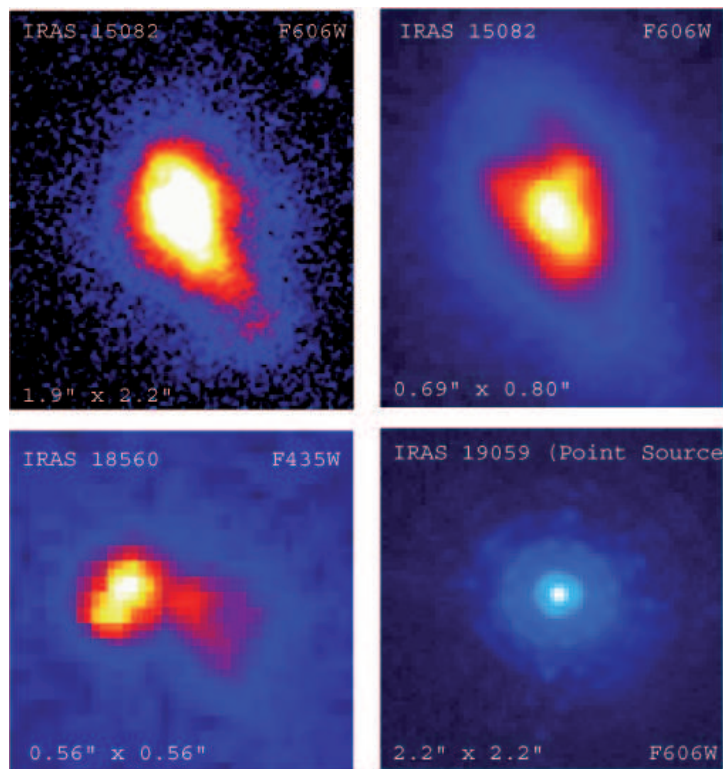


Fig. 4. as in Fig. 3. IRAS19059 is unresolved and represents the PSF

the fast outflow from V Hydrae). Understanding the properties of these outflows and their launch mechanism(s) is key to making progress in understanding the shaping of aspherical PNe.

References

1. Balick, B. 1987, AJ, 94, 671
2. Balick, B., Preston, H. L., & Icke, V. 1987, AJ, 94, 1641
3. Bujarrabal, V., Castro-Carrizo, A., Alcolea, J., & Sánchez Contreras, C. 2001, A&A, 377, 868
4. Claussen, M. J., Sahai, R., & Morris, M. 2007, *this proceedings*
5. Danchi, W. C., Tuthill, P. G., Bester, M., Lipman, E. A., Monnier, J. M., & Townes, C. H. 1998, *Cool Stars, Stellar Systems, and the Sun*, 154, 361
6. Dyck, H. M., Zuckerman, B., Leinert, C., & Beckwith, S. 1984, ApJ, 287, 801
7. Frank, A., Balick, B., Icke, V., & Mellema, G. 1993, ApJ, 404, L25
8. Hirano, N., et al. 2004, ApJ, 616, L43
9. Icke, V., Balick, B., & Frank, A. 1992, A&A, 253, 224

10. Ivezić, Z., Nenkova, M., & Elitzur, M. 1999, Univ. Kentucky Internal Report, arXiv:astro-ph/9910475
11. Knapp, G.R., Jorissen, A. & Young, K. 1997, A&A, 326, 318
12. Kwok, S., Purton, C. R., & Fitzgerald, P. M. 1978, ApJ, 219, L125
13. Lagadec, E., Mékarnia, D., de Freitas Pacheco, J. A., & Dougados, C. 2005, A&A, 433, 553
14. Lagadec, E., Chesneau, O., Zijlstra, A. A., Matsuura, M., & Mékarnia, D. 2007, *this proceedings*
15. Monnier, J. D., Tuthill, P. G., & Danchi, W. C. 2000, ApJ, 545, 957
16. Morris, M. 1987, PASP, 99, 1115
17. Sánchez Contreras, C., Le Mignant, D., Sahai, R., Gil de Paz, A., & Morris, M. 2007, ApJ, 656, 1150
18. Ragland, S., et al. 2006, ApJ, 652, 650
19. Soker, N., & Livio, M. 1989, ApJ, 339, 268
20. Sahai, R. & Wannier, P. G. 1985, ApJ, 299, 424
21. Sahai, R. & Wannier, P.G. 1988, A&A, 201, L9
22. Sahai, R., & Trauger, J. T. 1998, AJ, 116, 1357
23. Sahai, R., et al. 1998, ApJ, 493, 301
24. Sahai, R., Morris, M., Knapp, G. R., Young, K., & Barnbaum, C. 2003, Nature, 426, 261
25. Sahai, R., Morris, M., Sánchez Contreras, C. & Claussen, M.J. 2007, AJ, (Dec 07 issue, in press)
26. Sahai, R., Morris, M., Sánchez Contreras, C. & Claussen, M.J. 2007, (in prep)
27. Schmidt, G. D., Hines, D. C., & Swift, S. 2002, ApJ, 576, 429
28. Skinner, C. J., Meixner, M., & Bobrowsky, M. 1998, MNRAS, 300, L29
29. Soker, N. 1992, ApJ, 389, 628
30. Tuthill, P. G., Monnier, J. D., Danchi, W. C., & Lopez, B. 2000, ApJ, 543, 284
31. Weiner, J., et al. 2006, ApJ, 636, 1067